Journal of Medicinal Chemistry

Volume 50, Number 16 August 9, 2007

Articles

Synthesis and Biological Activity of Azido Analogues of 5,6-Dimethylxanthenone-4-acetic Acid for Use in Photoaffinity Labeling

Brian D. Palmer,[†] Kimiora Henare,[†] See-Tarn Woon,[†] Rachel Sutherland,[†] Charu Reddy,[†] Liang-Chuan S. Wang,[†] Claudine Kieda,[‡] and Lai-Ming Ching*[,†]

Auckland Cancer Society Research Centre, Faculty of Medical and Health Sciences, University of Auckland, Auckland, New Zealand, and Centre de Biophysique Moleculaire, UPR 4301 CNRS, Orleans Cedex, France

Received February 24, 2007

5,6-Dimethylxanthenone-4-acetic acid (**1**) is scheduled for phase III clinical trials as a vascular disrupting agent. However, its biochemical receptor(s) have yet to be identified. In this report, the synthesis of azido analogues of **1** that could be used for photoaffinity labeling of proteins as an approach toward identifying its molecular targets is described. While 5-azidoxanthenone-4-acetic acid (**2**) and 5-azido-6-methylxantheone-4-acetic acid (**3**) were found to have biological activities similar to that of **1**, 6-azido-5-methylxanthenone-4-acetic acid (**4**) was unstable and could not be evaluated. Both azido compounds **2** and **3** activated NF-κB, induced the production of tumor necrosis factor in cultured mouse splenocytes, and induced hemorrhagic necrosis of colon 38 tumors in mice. Photoreaction of lysates from spleen cells with tritiated **2** resulted in two radiolabeled protein bands at 50 and 14 kDa that could be competitively inhibited with cold **1** and cold **2**. The azido compounds **2** and **3** exhibit all the requirements for use in photoaffinity labeling of potential receptor(s) for **1**.

Introduction

A number of vascular disrupting agents are in the clinic for the treatment of cancer, most notably bevacizumab, a monoclonal antibody against the vascular endothelial growth factor, which has shown activity for colorectal cancers.[1−4] Combretastatin, the taxanes, and vinca alkaloids all cause antivascular effects through a disruption of normal polymerization of tubulin.[5−7] 5,6-Dimethylxanthenone-4-acetic acid (**1**) (DMXAA, AS1404), a synthetic small molecule that is scheduled to enter phase III clinical trial as a vascular disrupting agent, has a distinct mode of action that does not appear to involve tubulin as the main target (Figure 1). The molecular mode of action of **1** is not yet fully elucidated and may involve multiple pathways, depending on the cell type and context. In preclinical studies, **1** at its maximum tolerated dose (MTD) caused rapid and irreversible inhibition of tumor blood flow,[8,9] and the resultant ischemia and subsequent necrosis could account for the killing of nearly 90% of the tumor cells in established, vascularized

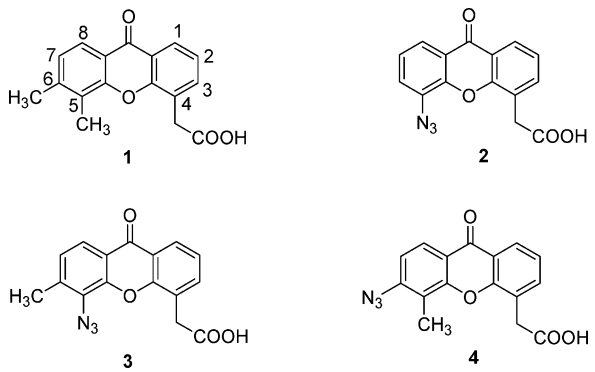

Figure 1. Chemical structures of 5,6-dimethylxantheone-4-acetic acid (**1**) and its azido analogues.

* To whom correspondence should be addressed. Phone: +64-9-3737-599, extension 86140. Fax: +64-9-3737-502. E-mail: l.ching@auckland.ac.nz.
[†] University of Auckland.
[‡] Centre de Biophysique Moleculaire.

10.1021/jm0702175 CCC: $37.00
Published on Web 07/06/2007

implants.[8] Selective apoptosis of vascular endothelial cells in colon 38 tumors was observed within 30 min of **1** administration,[10,11] and a significant correlation between the induction of vascular endothelial cell apoptosis and the reduction of tumor blood flow was obtained.[11] Maintenance of the tumor vascular collapse such that widespread necrosis develops involves the induction of a cascade of vasoreactive mediators such as serotonin,[12] nitric oxide,[13] and tumor necrosis factor (TNF) and other cytokines.[14−16]

The addition of inhibitors of IκB, parthenolide and salicylate, results in loss of production of TNF and IFN-γ in primary splenocyte cultures, indicating a role for NF-κB.[17] On the other hand, induction of apoptosis of human umbilical cord vein endothelial cells by **1** can occur in the absence of NF-κB activation, indicating alternative signaling pathways may predominate for **1**'s effects on endothelial cells.[18] One implication of the multiplicity of pathways that are involved in its action is that **1** may possess more than one cellular target, and approaches toward identification of its receptor(s) must take this complexity into account. The method of photoaffinity labeling would allow cellular proteins to be screened for binding to a photoreactive analogue of **1**, a technique that has been used successfully to identify protein targets for a number of other anticancer agents including verapamil,[19] paclitaxel,[20−22] and thalidomide.[23] We have previously shown that tritiated **1** associates only weakly to cell lysates, suggesting that it has a low affinity of binding to its receptor(s).[24] With this in mind, the use of a photoaffinity-labeling approach to the identification of its receptor was considered appropriate, since the probe becomes covalently attached to the target protein(s)[25] by use of this technique. Of course, low affinity binding of **1** could also lead to nonspecific labeling of many proteins and the formation of false positives, and so all identified proteins would have to be subsequently evaluated for their receptor status.

In this paper we describe the synthesis and biological activity of azido analogues (**2**−**4**) of **1** that could be used for photoaffinity labeling and subsequent identification of potential receptor(s) for **1**. We chose to use an azide group as the photoreactive substituent because it is readily introduced via diazotization of an aromatic amine, it is not as sterically demanding as alternative photoreactive groups, and it undergoes efficient conversion to a reactive nitrene species upon photolysis. Others have used aryl diazirine, aryl ketone, and diazoester groups for this purpose.[26] Tritiation of the selected photoprobe was used to introduce a reporter tag suitable for detection of probe−protein adducts.

Chemistry

Previous structure−activity relationship (SAR) studies of the activity of substituted xanthenone-4-acetic acids indicated a clear preference for substitution at the 5 and 6 positions of the ring system, with 5,6-disubstitution providing particularly potent compounds.[27] 5,6-Dimethylxanthenone-4-acetic acid (**1**) was chosen from among these for clinical evaluation. In these studies the 5-amino compound (**5**) displayed some activity in inducing hemorrhagic necrosis in colon 38 tumors, albeit at a significantly higher optimum dose than **1**.[28] These earlier SAR studies suggested that the 5 and 6 positions of the xanthenone-4-acetic acid ring system would be best for incorporation of azide functionality in order to retain a spectrum of biological activity similar to that of **1**. The 5-azido analogue (**2**) of **5** was prepared in good yield from **5** by conversion to the diazonium salt, followed by reaction with aqueous sodium azide (Scheme 1).

The methylated azides **3** and **4** were similarly prepared from the corresponding amino compounds **13** and **21** (Scheme 2).

Scheme 1[a]

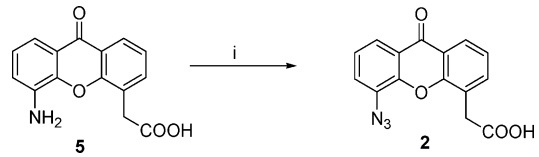

[a] Reagents and conditions: (i) $NaNO_2$, aqueous H_2SO_4, 0−5 °C, 10 min, then aqueous NaN_3, 0−5 °C, 1 h.

These were obtained by reduction of the nitroxanthenones **12** and **20**, which were prepared using chemistry similar to that developed in the original studies for construction of the xanthenone-4-acetic acid ring system.[28] Thus, the methylnitroanilines **6** and **14** were converted into isatins **8** and **16** using a recent modification of the isonitrosoacetanilide Sandmeyer procedure.[29] Oxidation to the anthranilic acids **9** and **17** followed by diazotization and reaction with KI gave iodides **10** and **18**. The potassium salt of these acids reacted with the disodium salt of 2-hydroxyphenylacetic acid under TDA-1 catalysis to give the diphenyl ethers **11** and **19**, which were cyclized to give the xanthenones **12** and **20** using 85% H_2SO_4. While the 5-azido compounds **2** and **3** were stable at room temperature, the 6-azido compound **4**, which has the azido group in resonance with the carbonyl group of the xanthenone ring, was moderately unstable under the same conditions, with decolorization occurring on standing (particularly in solution) and the formation of polar, baseline products by TLC analysis. For this reason, the azide **4** was considered to be unsuitable for tritiation and for further use as a probe.

Biological Activity

Induction of Hemorrhagic Necrosis. A hallmark of the antivascular effects of **1** is the induction of hemorrhagic necrosis of subcutaneously growing solid tumors in mice within 24 h of a single injection at the MTD.[30−32] The azido analogues were examined for their ability to induce hemorrhagic necrosis. Mice with colon 38 tumors were injected intraperitoneally with **1**, **2**, or **3** at respective MTDs of 25, 200, and 190 mg/kg. After 24 h, mice were killed and the tumor was excised. The histologies of all tumors were compared with those of untreated tumors, and a representative field of the untreated and treated tumors is shown in Figure 2. Untreated tumors had less than 5% necrosis, and tumors treated with all drugs exhibited greater than 95% hemorrhagic necrosis. Thus, all three agents had the ability to cause widespread necrosis, although the azido analogues were 8-fold lower in potency than **1**.

Cytotoxicity of the Azido Analogues Compared with 1. The direct cytotoxicity of the analogues compared with **1** on HECPP murine endothelial cells was measured using the MTT assay. Varying concentrations of each compound were added to cultures of HECPP murine endothelial cells, and the percent of metabolically active cells in culture was assessed after 24 h (Figure 3). Increasing concentrations of each drug led to a decrease in cell viability. The azido analogues were more cytotoxic than **1** in vitro, and the concentration required to cause 50% reduction in cell viability was 600 and 300 μg/mL, respectively, for **2** (Figure 3B) and **3** (Figure 3C), compared with 1000 μg/mL for **1** (Figure 3A).

Activation of NF-κB. 1 has been shown to activate NF-κB in a number of cell lines in culture[24,33] as well as in vivo in tumors,[34] although the precise role of the activated NF-κB in the action of **1** is not clear. The ability of **2** and **3** to also activate NF-κB in HECPP cells was investigated as an indication that the azido analogues share a spectrum of biological activity

Scheme 2[a]

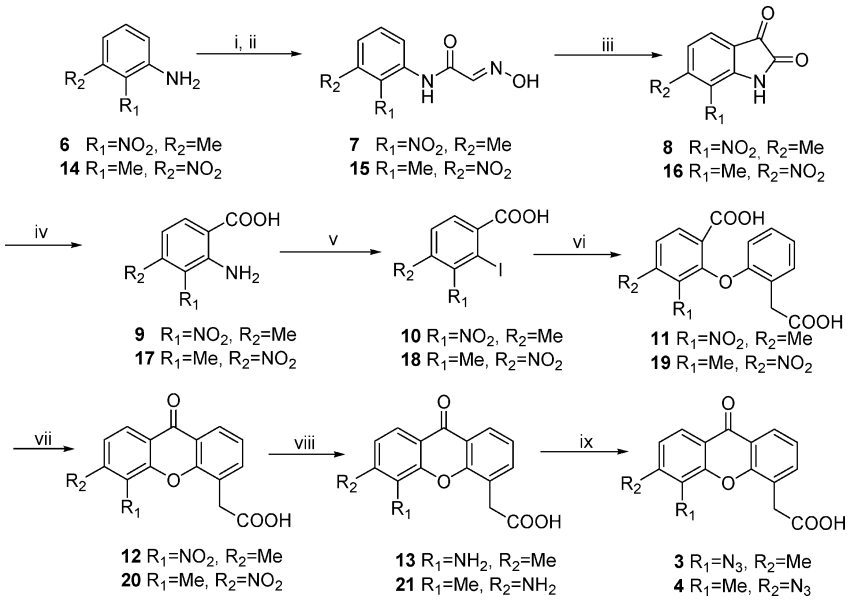

[a] Reagents and conditions: (i) $(AcO)_2CHCOCl$, $KHCO_3$, DCM, 20 °C, 1 h; (ii) $H_2NOH{\cdot}HCl$, EtOH−H_2O, reflux, 90 min; (iii) concentrated H_2SO_4, 80−93 °C, 30−150 min; (iv) H_2O_2, aqueous KOH, KCl, 20 °C, 2 h; (v) $NaNO_2$, concentrated H_2SO_4−85% H_3PO_4, 0−10 °C, 30 min, then aqueous KI, CuI, 10−80 °C, 10 min; (vi) 1 equiv of aqueous KOH, 20 °C, 5 min, dry well, then 2-hydroxyphenylacetic acid disodium salt, TDA-1, CuCl, *p*-dioxane, reflux, 16 h; (vii) 80% H_2SO_4, 80 °C, 15 min; (viii) H_2, 5% Pd−C, MeOH−EtOAc, 60 psig, 2 h; (ix) $NaNO_2$, aqueous H_2SO_4, 0−5 °C, 5 min, then aqueous NaN_3, 5−20 °C, 1.5 h.

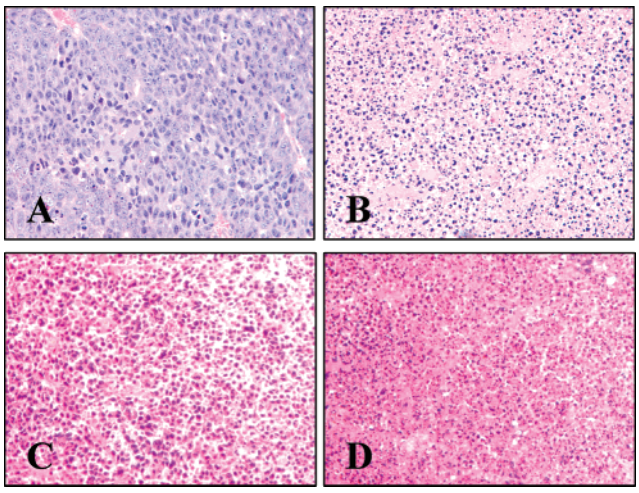

Figure 2. Histology of colon 38 tumor section (A) untreated or 24 h after treatment with (B) **1** (25 mg/kg), (C) **2** (200 mg/kg), or (D) **3** (190 mg/kg).

similiar to that of **1**. NF-κB was activated with **1** at 10 μg/mL and above (Figure 4A). With **2**, activated NF-κB was observed at 300 and 1000 μg/mL (Figure 4B), indicating a 30-fold lower potency than **1** in this activity. Activated NF-κB was observed with **3** at 30 and 100 μg/mL (Figure 4C), but no determinations could be obtained at higher doses because it was found to be toxic and sufficient amounts of nuclear extracts could not be obtained for testing.

Cytokine Induction in Murine Splenocyte Cultures. A key component of the action of **1** is the induction of cytokines, and we have previously used primary splenocyte cultures as an in vitro model for investigating this action of **1**.[35] The ability of the azido analogues to induce TNF in murine splenocyte cultures was compared with that of **1** (Figure 5). Both azido analogues induced TNF secretion into the culture supernatants, but clearly **1** was more active. Maximal TNF production (180 pg/mL) was obtained at 10 μg/mL of **1**, whereas **2** maximally induced 110 pg/mL TNF at 100 μg/mL. TNF production was obtained with **3** at 30 and 100 μg/mL only, and less than 50 pg/mL TNF was induced.

Photoaffinity Labeling and Specificity of Binding. Both azido compounds had similar activity and potency to each other. The less toxic 5-azidoxanthenone-4-acetic acid (**2**) was chosen for custom tritiation and evaluated for its utility in photoaffinity labeling. Lysates from murine splenocyte were incubated with tritiated **2** and then UV-irradiated. Other aliquots of cell lysates were preincubated with cold **1** or cold **2** before the addition of tritiated **2** and photoreaction. Parts A and B of Figure 6 show the Coomassie Blue stained gel and the autoradiograph, respectively. Two bands (50 and 14 kDa) were visible in the autoradiograph. More intense banding pattern was observed in lane 2 (UV-treated) compared to lane 1 (no UV treatment), indicating that photoactivation had induced binding between [^{3}H]-**2** and the proteins. Cold **1** reduced the radioactive intensity of the 14 kDa band (Figure 6B, lanes 3 and 4) but not that of the 50 kDa band. Excess cold **2**, however, was shown to competitively inhibit [^{3}H]-**2** from reacting with proteins in both the 50 and the 14 kDa bands (lane 6, Figure 6B).

Discussion and Conclusion

As shown in Figure 2, 5-azidoxanthenone-4-acetic acid (**2**) and 5-azido-6-methylxanthenone-4-acetic acid (**3**) retained the ability to cause profound necrosis of subcutaneously growing colon 38 in mice, a hallmark of the in vivo antitumor response to **1**. The two stable azido analogues were both less potent than **1**. Their MTDs in mice were approximately 8-fold higher than that for **1**, but at their respective MTDs, the degree of necrosis induced with the azido analogues was equivalent to that induced with **1** (Figure 2). The in vivo antitumor activity of this class of agents does not correlate with their in vitro cytotoxicity.[36] Excellent correlations are observed, however, between in vivo induction of tumor necrosis and in vitro activation of NF-κB[37] and enhancement of immune effector cell activity.[36,38] The biological evaluations here were consistent with previous observations. Although their MTDs in vivo were 8-fold higher,

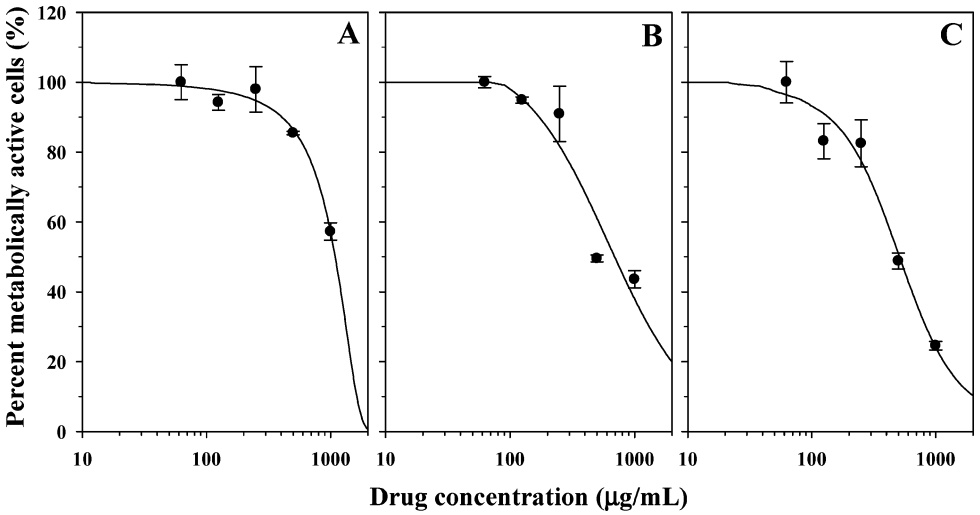

Figure 3. Percent survival of HECPP cells in culture 24 h after the addition of varying concentrations of (A) **1**, (B) **2**, or (C) **3**.

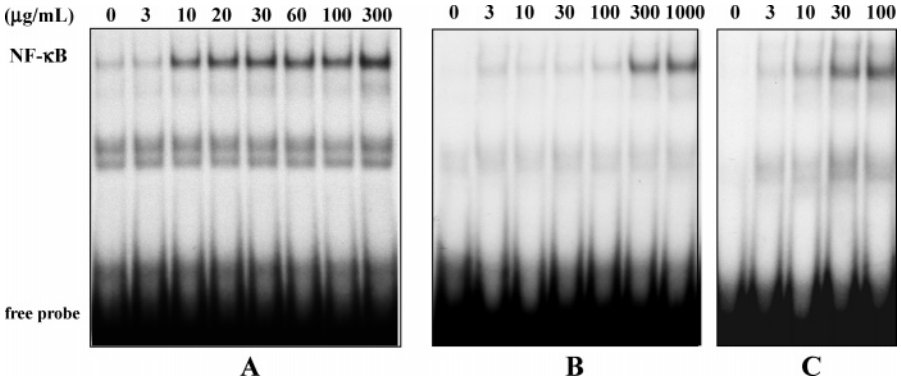

Figure 4. EMSA showing activated NF-κB in nuclear extracts from HECPP cells cultured for 2 h with indicated concentrations of (A) **1**, (B) **2**, or (C) **3**.

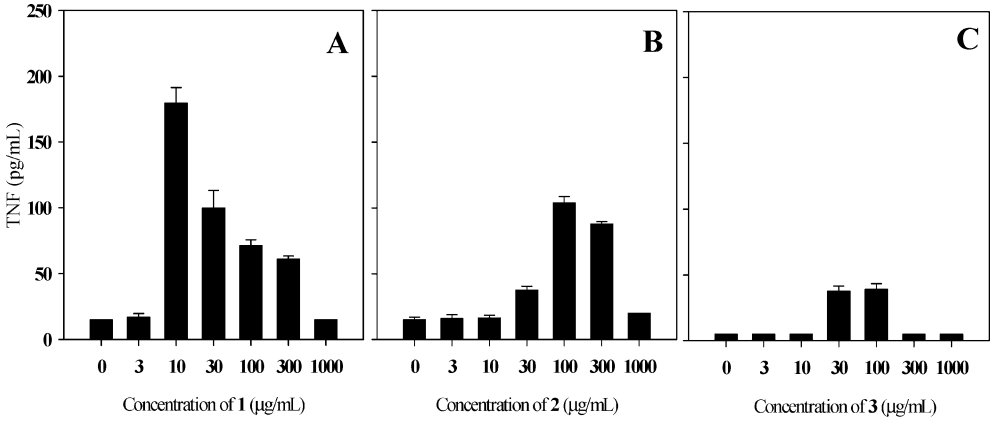

Figure 5. TNF activity in murine splenocyte culture supernatants 4 h after treatment with indicated concentrations of (A) **1**, (B) **2**, or (C) **3**.

the azido analogues were more toxic than **1** to cultured endothelial cells but were approximately 10-fold less potent than **1** in activating NF-κB (Figure 4) and in stimulating TNF production in cultured splenocytes (Figure 5). Despite differences in potencies, the results indicated that the azido compounds share a similar spectrum of biological effects as **1** and are therefore most likely to be acting on the same molecular targets as **1**. Moreover, compound **2** was shown to undergo photoreaction to specifically bind to cellular proteins extracted from murine splenocytes (Figure 6). We conclude that the two stable azidoxanthenone analogues **2** and **3** described in this report would be suitable for use in a photoaffinity approach to identify the receptor(s) for **1.**

Experimental Section

Chemistry. Combustion analyses were performed by the Microchemical Laboratory, University of Otago, Dunedin, NZ. Melting points were determined using an Electrothermal model 9200 digital melting point apparatus and are as read. NMR spectra were obtained on a Bruker Avance-400 spectrometer and are referenced to Me_4Si. APCI mass spectrometry was performed on a Surveyor MSQ single quadrupole spectrometer (ThermoFinnigan), using methanol

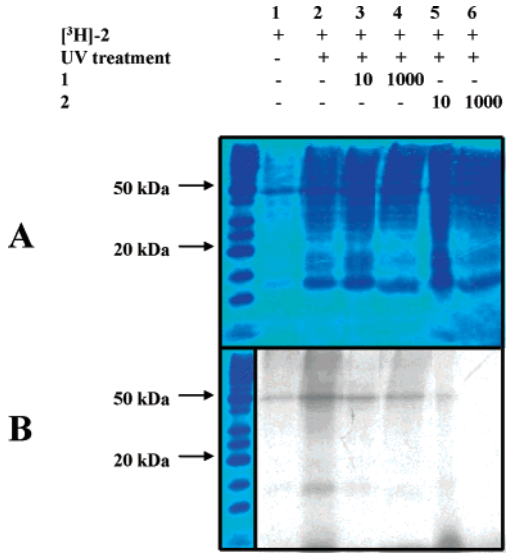

Figure 6. (A) SDS−PAGE gel of murine splenocyte proteins incubated with tritiated **2** without UV treatment (lane 1) and with UV treatment (lane 2), preincubated with 10- and 1000-fold excess of cold **1** (lanes 3 and 4, respectively), and preincubated with 10- and 1000-fold excess of cold **2** prior to UV treatment (lanes 5 and 6, respectively). (B) Autoradiograph of the gel showing radioactive protein bands at 50 and 14 kDa.

solutions and simultaneous positive and negative ion acquisition. Flash column chromatography was performed on silica gel 60 support (Scharlau, 230−400 mesh ASTM), using the indicated eluants.

(5-Azido-9-oxo-9*H*-xanthen-4-yl)acetic Acid (2). Concentrated H_2SO_4 (8 mL) was added to powdered amino compound **5**[28] (0.20 g, 0.74 mmol), which had been cooled to 5 °C in an ice bath. Stirring was continued until the mixture became homogeneous, and then an ice−water slurry (∼50 g) was added in one portion. The clear, colorless solution was recooled to 5 °C, and a solution of $NaNO_2$ (73 mg, 1.06 mmol) in water (5 mL) was added dropwise over 5 min. After the mixture was stirred for an additional 10 min at 0−5 °C, a solution of NaN_3 (0.28 g, 4.30 mmol) in cold water (10 mL) was added in one portion, and the mixture was stirred with cooling for 1 h. The white precipitate was filtered off, washed well with water, and air-dried to give the azide **2** as a white solid (0.21 g, 96%): mp 169 °C (dec); ^{1}H NMR ($(CD_3)_2SO$) δ 12.60 (br, 1 H), 8.12 (dd, J = 8.0, 1.7 Hz, 1 H), 7.98 (dd, J = 8.0, 1.6 Hz, 1 H), 7.84 (dd, J = 7.3, 1.7 Hz, 1 H), 7.71 (dd, J = 7.8, 1.6 Hz, 1 H), 7.50−7.45 (m, 2 H), 3.99 (s, 2 H). APCI found: $[M + H]^+ = 296$. Anal. ($C_{15}H_{19}N_3O_4$) C, H, N. The azide **2** was randomly tritiated in the xanthenone ring by SibTech, Inc., using a custom proprietary procedure.[39] The specific activity thus obtained was 0.1 mCi/mmol.

6-Methyl-7-nitro-1*H*-indole-2,3-dione (8). A solution of diacetoxyacetyl chloride (21.9 g, 0.113 mol) in dichloromethane (50 mL) was added dropwise to a vigorously stirred mixture of 2-nitro-3-methylaniline (**6**) (13.21 g, 0.086 mol) and $KHCO_3$ (43.5 g, 0.434 mol) in dichloromethane (200 mL) at −10 °C. After 5 min, the cooling bath was removed and the mixture was stirred at room temperature for 1 h. The solid material was removed by filtration, which was washed with dichloromethane. The combined dichloromethane solution was concentrated to dryness, and the residue was dissolved in ethanol (120 mL). A solution of hydroxylamine hydrochloride (30.2 g, 0.434 mol) in water (60 mL) was added, and the solution was refluxed for 90 min. The solvent was removed in vacuo and the residue was extracted with ethyl acetate, washed with water, then worked up to give the crude isonitrosoacetanilide **7** as an orange syrup (63%), which was used directly. Concentrated H_2SO_4 (80 mL) was added to crude **7** (10.0 g, 0.045 mol), and the mixture was warmed at 80 °C for 30 min. The resulting solution was cooled and poured onto crushed ice. The resulting brown solid was filtered off, washed with water, and dissolved in 1 N NaOH (200 mL). The pH was adjusted to 6 by the addition of acetic acid, and the resulting brown precipitate was removed by filtration. The filtrate was acidified by the addition of concentrated HCl and the precipitate was filtered off and washed well with water to give the isatin **8** as a yellow solid (3.33 g, 36%): mp (EtOH) 238 °C; ^{1}H NMR ($(CD_3)_2SO$) δ 1.39 (br s, 1 H), 7.69 (d, J = 7.6 Hz, 1 H), 7.13 (d, J = 7.6 Hz, 1 H), (2.50, s, 3H). Anal. ($C_9H_6N_2O_4 \cdot 0.25H_2O$) C, H, N.

7-Methyl-6-nitro-1*H*-indole-2,3-dione (16). Reaction of the isonitrosoacetanilide **15**[29] with concentrated H_2SO_4 as described above for the preparation of **8**, except that the reaction time was 2.5 h at a temperature of 93 °C, gave the isatin **16** (54%) as an orange powder: mp 148−151 °C; ^{1}H NMR ($(CD_3)_2SO$) δ 1.45 (br s, 1 H), 7.55 (d, J = 8.0 Hz, 1 H), 7.53 (d, J = 8.0 Hz, 1 H), 2.25 (s, 3 H). Anal. ($C_9H_6N_2O_4 \cdot 0.125H_2O$) C, H, N.

2-Amino-4-methyl-3-nitrobenzoic Acid (9). The isatin **8** (3.30 g, 0.016 mol) was dissolved in a solution of KOH (0.99 g, 0.018 mol) and KCl (2.5 g, 0.034 mol) in water (30 mL), and the solution was cooled to 10 °C. Hydrogen peroxide (3.3 g of a 27% aqueous solution, 0.026 mol) was added dropwise, and stirring was continued at this temperature for 5 min, then at room temperature for 2 h. The resulting orange suspension was acidified with acetic acid and the precipitate was filtered off and washed well with water to give **9** as a bright-yellow powder (2.71 g, 86%): mp (ethyl acetate/petroleum ether) 221−223 °C. ^{1}H NMR ($(CD_3)_2SO$) δ 7.87 (d, J = 8.1 Hz, 1 H), Anal. ($C_8H_8N_2O_4$) C, H, N.

2-Amino-3-methyl-4-nitrobenzoic Acid (17). Reaction of the isatin **16** with H_2O_2 exactly as described above for the isomer **8** gave the anthranilic acid **17** (68%) as a yellow solid: mp (ethyl acetate/petroleum ether) 208−211 °C; ^{1}H NMR ($CDCl_3$) δ 7.94 (d, J = 8.8 Hz, 1 H), 6.94 (d, J = 8.8 Hz, 1 H), 6.22 (br, 2 H), 2.22 (s, 3 H). APCI found: $[M - H]^- = 195$. Anal. ($C_8H_8N_2O_4$) C, H, N.

2-Iodo-4-methyl-3-nitrobenzoic Acid (10). The amine **9** (7.00 g, 0.036 mol) was dissolved in concentrated H_2SO_4 (130 mL), and the solution was cooled to 5 °C. A chilled solution of $NaNO_2$ (2.69 g, 0.039 mol) in concentrated H_2SO_4 (130 mL) was added dropwise with stirring, keeping the temperature below 10 °C. Chilled 85% H_3PO_4 (255 mL) was then added at such a rate that the temperature remained below 10 °C (this requires an acetone−dry ice bath), and stirring was continued for a further 30 min. The resulting tan suspension was poured onto an ice−water mixture, and a solution of KI (29.6 g, 0.18 mol) in water (150 mL) was added in one portion. CuI (25.6 g, 0.020 mol) was added, and the mixture was warmed to 80 °C. After 10 min at this temperature, ethyl acetate was added and the mixture was stirred well, then filtered through Celite. The ethyl acetate layer was removed from the filtrate, washed with aqueous sodium sulfite solution, then water, and worked up to give an orange solid, which was slurried with hot benzene to leave the iodide **10** as a tan powder (6.53 g, 59.5%). A portion crystallized from aqueous methanol as a cream solid: mp 244 °C; ^{1}H NMR ($(CD_3)_2SO$) δ 13.8 (br, 1 H), 7.72 (d, J = 7.9 Hz, 1 H), 7.54 (d, J = 7.9 Hz, 1 H), 2.31 (s, 3 H) (COOH resonance not visible). APCI found: $[M - H]^- = 306$. Anal. ($C_8H_6INO_4 \cdot 0.25MeOH$) C, H, N.

2-Iodo-3-methyl-4-nitrobenzoic Acid (18). Reaction of the anthranilic acid **17** exactly as described above for the isomer **9** gave the iodide **18** (84%) as a tan powder: mp (benzene/petroleum ether) 168−172 °C; ^{1}H NMR ($(CD_3)_2SO$) δ 13.80 (br, 1 H), 7.91 (d, J = 8.3 Hz, 1 H), 7.52 (d, J = 8.3 Hz, 1 H), 2.52 (s, 3 H). APCI found: $[M - H]^- = 306$. Anal. ($C_8H_6INO_4 \cdot 0.25C_6H_6$) C, H, N.

2-[2-(Carboxymethyl)phenoxy]-4-methyl-3-nitrobenzoic Acid (11). To a solution of the acid **10** (6.53 g, 0.021 mol) in methanol (300 mL) was added 1 N KOH (21 mL, 0.02 mol). After 5 min the solution was concentrated to dryness and dried well in a vacuum oven to leave the potassium salt of the acid as a colorless powder. *p*-Dioxane (500 mL) was added, followed by the disodium salt of 2-hydroxyphenylacetic acid (4.94 g, 0.025 mol), TDA-1 (0.81 g, 2.52 mmol), and CuCl (0.25 g, 2.52 mmol), and the mixture was

refluxed under nitrogen for 16 h. The solvent was removed in vacuo, and the residue was dissolved in 1 N NaOH (500 mL) and filtered. The filtrate was acidified with concentrated HCl, and the solution was extracted with ethyl acetate. The extract was dried and concentrated to ~50 mL. Addition of petroleum ether precipitated the ether **11** as a brown powder sufficiently pure for the next step (3.25 g, 46%). A small portion was recrystallized from aqueous acetone to give **11** as a fine, tan powder: mp 220−221 °C; ^{1}H NMR ($(CD_3)_2SO$) δ 13.8−11.0 (br, 2 H), 7.97 (d, J = 8.1 Hz, 1 H), 7.49 (d, J = 8.1 Hz, 1 H), 7.30 (dd, J = 7.5, 1.5 Hz, 1 H), 7.12 (ddd, J = 7.73, 7.4, 1.5 Hz, 1 H), 7.0 (ddd, J = 7.5, 7.4, 1.5 Hz, 1 H), 6.28 (d, J = 7.7 Hz, 1 H), 3.65 (br s, 2 H), 2.36 (s, 3 H). APCI found: $[M - H]^-$ = 330. Anal. ($C_{16}H_{13}NO_7$) C, H, N.

2-[2-(Carboxymethyl)phenoxy]-3-methyl-4-nitrobenzoic Acid (19). Reaction of the potassium salt of the iodide **18** with the disodium salt of 2-hydroxyphenyl acetic acid, exactly as described above for the isomeric iodide **10**, gave the diphenyl ether **19** (51%) as tan cubes: mp (ethyl acetate/petroleum ether) 228−232 °C; ^{1}H NMR ($(CD_3)_2SO$) δ 12.15 (br, 2 H), 7.97 (d, J = 8.2 Hz, 1 H), 7.49 (d, J = 8.2 Hz, 1 H), 7.29 (dd, J = 7.5, 1.5 Hz, 1 H), 7.13 (ddd, J = 8.02, 7.5, 1.5 Hz, 1 H), 6.99 (ddd, J = 8.0, 7.5, 0.9 Hz, 1 H), 6.38 (dd, J = 7.5, 0.9 Hz, 1 H), 3.65 (br s, 2 H), 2.37 (s, 3 H). APCI found: $[M - H]^-$ = 330. Anal. ($C_{16}H_{13}NO_7$) C, H, N.

(5-Amino-6-methyl-9-oxo-9*H*-xanthen-4-yl)acetic Acid (13). A solution of the diacid **11** (3.20 g, 9.66 mmol) in 80% H_2SO_4 (v/v, 30 mL) was warmed at 80 °C for 15 min. The cooled solution was poured onto crushed ice, which was diluted further with water. The brown precipitate was filtered off, adsorbed onto silica from an ethyl acetate solution, and chromatographed on silica. Elution with ethyl acetate−petroleum ether (1:1) gave foreruns, while ethyl acetate eluted the nitroxanthenone **12** as a tan powder (0.75 g, 25%). The material was immediately dissolved in ethyl acetate−methanol (1:1) (60 mL) and hydrogenated over 5% Pd−C (30 mg) at 60 psi for 2 h. The catalyst was filtered off and the filtrate concentrated to give a yellow solid, which was slurried in methanol to leave **13** as a pale-yellow solid (0.57 g, 21% overall from **11**): mp 242−246 °C; ^{1}H NMR ($(CD_3)_2SO$) δ 12.50 (br, 1 H), 8.90 (dd, J = 8.0, 1.7 Hz, 1 H), 7.78 (dd, J = 7.2, 1.7 Hz, 1 H), 7.40 (dd, J = 8.0, 7.2 Hz, 1 H), 7.34 (d, J = 8.0 Hz, 1 H), 7.12 (d, J = 8.0 Hz, 1 H), 5.25 (br s, 2 H), 4.02 (s, 2 H), 2.29 (s, 3 H). APCI found: $[M + H]^+$ = 284. Anal. ($C_{16}H_{13}NO_4$) C, H, N.

(6-Amino-5-methyl-9-oxo-9*H*-xanthen-4-yl)acetic Acid (21). Cyclization of the diacid **19** with 80% H_2SO_4 followed by immediate reduction of the resulting nitroxanethenone **20**, exactly as described above for the isomeric diacid **11**, gave crude product **21** which was purified by chromatography on silica. Elution with 5% methanol in ethyl acetate gave the amino compound **21** as a pale-yellow powder (32% overall yield from **19**): mp 290−293 °C; ^{1}H NMR ($(CD_3)_2SO$) δ 7.95 (dd, J = 8.0, 1.7 Hz, 1 H), 7.74 (d, J = 8.7 Hz, 1 H), 7.61 (dd, J = 7.3, 1.7 Hz, 1 H), 7.27 (dd, J = 8.7, 7.3 Hz, 1 H), 66.71 (d, J = 8.7 Hz, 1 H), 6.19 (br, 2 H), 3.77 (br s, 2 H), 2.19 (s, 3 H). APCI found: $[M + H]^+$ = 284. Anal. ($C_{16}H_{13}NO_4 \cdot 0.125H_2O$) C, H, N.

(5-Azido-6-methyl-9-oxo-9*H*-xanthen-4-yl)acetic Acid (3). Concentrated H_2SO_4 (10 mL) was added to the powdered amine **13** (0.23 g, 0.832 mmol), and the resulting solution was immediately cooled in an ice bath. After 2 min, ice−water (60 g) was added in one portion and the mixture was stirred until the internal temperature was 3 °C. A small amount of insoluble material was removed by filtration, and the solution was recooled to 3 °C. A solution of NaN_3 (63 mg, 0.91 mmol) in water (0.5 mL) was added dropwise. After the mixture was stirred for 5 min, a solution of NaN_3 (0.30 g, 4.61 mmol) in water (2 mL) was added, and the mixture was stirred at 3 °C for 30 min, then at room temperature for 1 h. The resulting solid was filtered off, washed well with water, and dried in vacuo to give the azide **3** as a cream powder (0.23 g, 92%): mp 160−163 °C (dec); ^{1}H NMR ($(CD_3)_2SO$) δ 8.14 (dd, J = 7.9, 1.7 Hz, 1 H), 7.91 (d, J = 8.1 Hz, 1 H), 7.83 (dd, J = 7.3, 1.7 Hz, 1 H), 7.48 (dd, J = 7.9, 7.3 Hz, 1 H), 7.36 (d, J = 8.1 Hz, 1 H), 4.03 (s, 2 H), 2.41 (s, 3 H). APCI found: $[M + H]^+$ = 310 (60%), 282 (100%). Anal. ($C_{16}H_{11}N_3O_4 \cdot 0.5H_2O$) C, H, N.

(6-Azido-5-methyl-9-oxo-9*H*-xanthen-4-yl)acetic Acid (4). Diazotization of the amino compound **21**, followed by reaction with NaN_3 exactly as described above for the isomeric amine **13**, gave the azide **4** as a tan solid (85%): mp, slowly sintered upon heating. This material was unstable at room temperature, especially when in solution, gradually discoloring and forming polar products on standing over several hours. The compound could be stored at −30 °C for at least 6 months. ^{1}H NMR ($(CD_3)_2SO$) δ 8.13−8.07 (m, 2 H), 7.80 (d, J = 7.2 Hz, 1 H), 7.47−7.40 (m, 2 H), 3.90 (s, 2 H), 2.34 (s, 3 H). APCI found: $[M + H]^+$ = 310.

Biology. Mice and Reagents. C57Bl/6 mice were bred at the Animal Research Unit, Auckland University, and were housed under conditions of constant temperature, lighting, and humidity. All experiments used male mice, 8−12 weeks old, and conformed to local institutional guidelines. The sodium salt of **1**, synthesized at the Auckland Cancer Society Research Centre,[27] was dissolved in culture medium for in vitro experiments and saline for injections into mice.

Determination of Hemorrhagic Necrosis. Colon 38 adenocarcinoma fragments (~1 mm^3) were subcutaneously implanted into the left flank of anesthetized (sodium pentobarbital, 82 mg/kg) mice and allowed to grow to a diameter of approximately 5 × 6 mm, which generally required 14 days. Groups of colon 38 tumor-bearing mice were administered with **1** (25 mg/kg), **2** (200 mg/kg), or **3** (190 mg/kg) by intraperitoneal injection, while another group was left untreated. Twenty-four hours after treatment, tumors were excised from the mice immediately after cervical dislocation, fixed in formalin, sectioned, and stained with hematoxylin and eosin. A section across the major axis of the tumor was examined on a grid marked at 0.4 mm intervals and was scored for percentage of necrosis as previously described.[12] At least three mice were used for each treatment group.

Cell Culture. All cultures were maintained at 37 °C under humidified atmosphere of 5% CO_2 in air. HECPP murine endothelial cells[40] were cultured in M199 medium (Gibco BRL Life Technologies, Gaithersburg, MD) supplemented with 10% fetal calf serum (FCS), 100 U/mL ampicillin, and 100 μg/mL streptomycin.

Splenocytes were obtained from mice following cervical dislocation. Spleens were removed and the cells squeezed out from the capsule into 10 mL of culture medium (Alpha-MEM supplemented with 10% FCS, 100 U/mL ampicillin, and 100 μg/mL streptomycin). Spleen cells were aspirated to form a single cell suspension, and red blood cells were removed by osmotic lysis. Nucleated cells were counted using a hemocytometer, and the cell concentration was adjusted to 3 × 10^7 cells/mL. Murine splenocytes were cultured in flat-bottomed 96-well plates at 3 × 10^6 cells/well, with drugs in a total volume of 200 μL of culture medium. After the appropriate incubation period, which was 4 h for the majority of the experiments, 150 μL of the supernatant from each well was removed and stored at −20 °C until analyzed for cytokines.

Cytotoxicity Assay. The MTT (3-(4,5-cimethylthiazol-2-yl)-2,5-diphenyltetrazolium bromide) colorimetric assay was used to assess loss of cell viability in culture.[41] HECPP cells were seeded in flat-bottomed 96 well plates at a density of 10^5 cells/well in 100 μL and incubated overnight. Drugs were added the following day, and after a further 24 h of incubation, MTT (10 μL of a solution of 5 mg/mL in PBS) was added to each well. The cells were incubated for a further 2 h to allow living cells to cleave the pale-yellow MTT substrate and form dark-blue formazan crystals. The formazan crystals in the cells were dissolved by the addition of 100 μL of 0.04 N HCl/isopropanol, and the absorbance in each well was measured with a microplate reader at 550 nm with a 630 nm reference filter.

Measurement of TNF. Supernatants from splenocytes cultures were collected 4 h after drug treatment and assayed for the presence of TNF using commercially available ELISA kits (OptEIA Mouse TNF-α Kit, Pharmingen, San Diego, CA), following the manufacturer's instructions. Each sample was assayed in duplicate, and

triplicate wells were set up for each test condition. The mean ± SEM values were calculated.

Preparation of Nuclear Extracts and Assay for Activated NF-κB. HECPP cells (2.5×10^7) were incubated with **1** or azido analogues and harvested after 2 h. Nuclear proteins were prepared as previously described.[35] Cells were lysed in cell lysis buffer (15 mM KCl, 10 mM HEPES (pH 7.6), 2 mM $MgCl_2$, 0.1 mM EDTA, 25 μM dithiothreitrol (DTT), 25 μM phenylmethylsulphonyl fluoride (PNPGB), and 0.5% Nonidet P-40) for 30 min. The pellet of nuclei was then incubated in 10 μL of nuclei lysis buffer (0.5 M KCl, 25 mM HEPES (pH 7.6), 0.1 mM EDTA, 1 mM DTT, 25 μM PNPGB) on ice for 30 min, and then 100 μL of dialysis buffer (25 mM HEPES, pH 7.6, 0.1 mM EDTA, 1 mM DTT, 10% glycerol, 25 μM PNPGB) was added. After centrifugation at 20000*g* for 15 min, the supernatant was collected and the protein concentration was determined with Bradford reagent at 596 nm.[42] NF-κB complexes in the nuclear extracts were determined using the electrophoretic mobility shift assay (EMSA) as previously described.[33] Briefly, the oligonucleotide (5′-AGCTTACAAGG-GACTTTC-3′) containing the NF-κB consensus binding site from the κ immunoglobulin enhancer gene,[43] annealed to its complementary strand, was radiolabeled using the Klenow fragment of DNA polymerase I (Klenow Fill-In Kit, Stratagene, La Jolla, CA) and [α-^{32}P]dCTP (370 mBq/mL, 10 mCi/mL, Redivue, Amersham) in a fill-in reaction for 5′-protruding ends. DNA binding reactions were carried out in total volume of 15 μL containing 5 μg of nuclear protein, 4 μL of binding buffer (20 mM KCl, 12 mM HEPES, pH 7.6, 2.5 mM $MgCl_2$, 0.4 mM EDTA, 0.5 mM DTT, 25 μM PNPGB, 12% glycerol), and 1.5 μg of poly(dI/dC). Samples were incubated on ice for 10 min before adding the ^{32}P-labeled probe (20 000 cpm). Reactions were terminated by the addition of a loading dye (250 mM Tris (pH 7.5), 0.2% bromophenol blue, 0.2% xylene cyanol, and 4% glycerol). Samples were loaded onto a 4% polyacrylamide gel and subjected to electrophoresis in 0.25× TBE buffer (22.3 mM Tris, 22.2 mM borate, 0.5 mM EDTA) at 150 V for 2 h. The dried gels were exposed to autoradiography (Kodak Scientific Imaging Film) at −80 °C overnight.

Preparation of Cell Lysate for Photoaffinity Labeling and 1D Gel Electrophoresis. Murine splenocytes (2×10^7) were lysed with Milli-Q water for 5 min and centrifuged (1100*g*, 10 min) to remove cell debris. Lysate (25 μg) was incubated with 1.8 μg of [^{3}H]-**2** (0.1 mCi/mmol, Sibtech, Inc., Newington, CT) in a volume of 10 μL. To test for specificity of binding, other aliquots were preincubated with 18 or 1800 μg of unlabeled **1** or **2** dissolved in Milli-Q water for 15 min on ice before the addition of [^{3}H]-**2**. After 5 min, the samples were UV-irradiated (254 nm, Stratlinker 1800, Stratagene, La Jolla, CA) for 2 min and then the proteins were separated by SDS gel electrophoresis. Each sample (15 μL) was mixed with sample buffer (15 μL (Laemmli sample buffer plus 5% of 2-mercaptoethanol), incubated at 98 °C for 4 min, and left at room temperature till loading. The sample mixture (20 μL) and prestained molecular weight protein standards (5 μL, Bio-Rad) were loaded onto the gel. Electrophoresis was carried out at 120 V until the dye front reached the bottom of the glass plates (90 min). The gel was then stained with Coomassie Blue (1 h) and destained with 40% methanol/5% acetic acid (1 h). The gel was then treated for 1 h with Amplify fluorographic solution (Amersham Pharmacia Biotech Inc, Piscataway, NJ). The gel was then transferred to 3MM filter paper, vacuum-dried for 1 h at 80 °C (model 583, Bio-Rad, Hercules, CA), and exposed at −80 °C for 1 month to detect protein bands with radioactivity. The autoradiograph was overlaid on the Coomassie Blue stained gel to identify the protein bands that were radioactive.

Acknowledgment. This work was funded by the Auckland Division of the New Zealand Cancer Society and Project Grant 05/237 from the Health Research Council of New Zealand.

Supporting Information Available: Combustion analysis data for all new compounds. This material is available free of charge via the Internet at http://pubs.acs.org.

References

(1) Lippert, J. W., 3rd. Vascular disrupting agents. *Bioorg. Med. Chem.* **2007**, *15*, 605−615.
(2) Gaya, A. M.; Rustin, G. J. S. Vascular disrupting agents: a new class of drug in cancer therapy. *Clin. Oncol.* **2005**, *17*, 277−290.
(3) Herbst, R. S.; Johnson, D. H.; Mininberg, E.; Carbone, D. P.; Henderson, T.; Kim, E. S.; Blumenschein, G., Jr.; Lee, J. J.; Liu, D. D.; Truong, M. T.; et al. Phase I/II trial evaluating the anti-vascular endothelial growth factor monoclonal antibody bevacizumab in combination with the HER-1/epidermal growth factor receptor tyrosine kinase inhibitor erlotinib for patients with recurrent non-small-cell lung cancer. *J. Clin. Oncol.* **2005**, *23*, 2544−2555.
(4) Sandler, A.; Gray, R.; Perry, M. C.; Brahmer, J.; Schiller, J. H.; Dowlati, A.; Lilenbaum, R.; Johnson, D. H. Paclitaxel−carboplatin alone or with bevacizumab for non-small-cell lung cancer. *N. Engl. J. Med.* **2006**, *355*, 2542−2550.
(5) Tozer, G. M.; Kanthou, C.; Baguley, B. C. Disrupting tumour blood vessels. *Nat. Rev. Cancer* **2005**, *5*, 423−435.
(6) Attard, G.; Greystoke, A.; Kaye, S.; De Bono, J. Update on tubulin-binding agents. *Pathol. Biol.* **2006**, *54*, 72−84.
(7) Pellegrini, F.; Budman, D. R. Review: tubulin function, action of antitubulin drugs, and new drug development. *Cancer Invest.* **2005**, *23*, 264−273.
(8) Zwi, L. J.; Baguley, B. C.; Gavin, J. B.; Wilson, W. R. The morphological effects of the anti-tumor agents flavone acetic acid and 5,6-dimethylxanthenone acetic acid on the colon 38 mouse tumor. *Pathology* **1994**, *26*, 161−169.
(9) Lash, C. J.; Li, A. E.; Rutland, M.; Baguley, B. C.; Zwi, L. J.; Wilson, W. R. Enhancement of the anti-tumour effects of the antivascular agent 5,6-dimethylxanthenone-4-acetic acid by combination with 5-hydroxytryptamine and bioreductive drugs. *Br. J. Cancer* **1998**, *78*, 439−445.
(10) Ching, L. M.; Cao, Z.; Kieda, C.; Zwain, S.; Jameson, M. B.; Baguley, B. C. Induction of endothelial cell apoptosis by the antivascular agent 5,6-dimethylxanthenone-4-acetic acid. *Br. J. Cancer* **2002**, *86*, 1937−1942.
(11) Ching, L. M.; Zwain, S.; Baguley, B. C. Relationship between tumour endothelial cell apoptosis and tumour blood flow shutdown following treatment with the antivascular agent DMXAA in mice. *Br. J. Cancer* **2004**, *90*, 906−910.
(12) Baguley, B. C.; Zhuang, L.; Kestell, P. Increased plasma serotonin following treatment with flavone-8-acetic acid, 5,6-dimethylxanthenone-4-acetic acid, vinblastine, and colchicine: relation to vascular effects. *Oncol. Res.* **1997**, *9*, 55−60.
(13) Thomsen, L. L.; Baguley, B. C.; Wilson, W. R. Nitric oxide: its production in host-cell-infiltrated EMT6 spheroids and its role in tumour cell killing by flavone-8-acetic acid and 5,6-dimethylxanthenone-4-acetic acid. *Cancer Chemother. Pharmacol.* **1992**, *31*, 151−155.
(14) Philpott, M.; Baguley, B. C.; Ching, L. M. Induction of tumour necrosis factor-alpha by single and repeated doses of the antitumour agent 5,6-dimethylxanthenone-4-acetic acid. *Cancer Chemother. Pharmacol.* **1995**, *36*, 143−148.
(15) Cao, Z.; Baguley, B. C.; Ching, L. M. Interferon-inducible protein 10 induction and inhibition of angiogenesis in vivo by the antitumor agent 5,6-dimethylxanthenone-4-acetic acid. *Cancer Res.* **2001**, *61*, 1517−1521.
(16) Perera, P. Y.; Barber, S. A.; Ching, L. M.; Vogel, S. N. Activation of LPS-inducible genes by the antitumor agent 5,6-dimethylxanthenone-4-acetic acid in primary murine macrophages. Dissection of signaling pathways leading to gene induction and tyrosine phosphorylation. *J. Immunol.* **1994**, *153*, 4684−4693.
(17) Wang, L.-C. S.; Woon, S.-T.; Baguley, B. C.; Ching, L.-M. Inhibition of DMXAA-induced tumor necrosis factor production in murine splenocyte cultures by NF-kappaB inhibitors. *Oncol. Res.* **2006**, *16*, 1−14.
(18) Woon, S-T; Hung, S. S.-C; Wu, D. C. F.; Schooltink, M. A.; Rachel Sutherland, R.; Baguley, B. C.; Chen, Q.; Chamley, L. W.; Ching, L.-M. NF-κB-independent induction of endothelial cell apoptosis by the vascular disrupting agent DMXAA. *Anticancer Res.*, in press.
(19) Safa, A. R. Photoaffinity labeling of the multidrug-resistance-related P-glycoprotein with photoactive analogs of verapamil. *Proc. Natl. Acad. Sci. U.S.A.* **1988**, *85*, 7187−7191.
(20) Rao, S.; Krauss, N.; Heerding, J.; Swindell, C.; Ringel, I.; Orr, G. A.; Horwitz, S. B. 3′-(*p*-Azidobenzamido)taxol photolabels the N-terminal 31 amino acids of beta-tubulin. *J. Biol. Chem.* **1994**, *269*, 3132−3134.
(21) Rao, S.; Orr, G. A.; Chaudhary, A. G.; Kingston, D. G. I.; Horwitz, S. B. Characterization of the Taxol binding site on the microtubule. *J. Biol. Chem.* **1995**, *270*, 20235−20238.

(22) Rao, S.; He, L.; Chakravarty, S.; Ojima, I.; Orr, G. A.; Horwitz, S. B. Characterization of the Taxol binding site on the microtubule. Identification of Arg282 in beta-tubulin as the site of photoincorporation of a 7-benzophenone analog of Taxol. *J. Biol. Chem.* **1999**, *274*, 37990−37994.
(23) Turk, B. E.; Jiang, H.; Liu, J. O. Binding of thalidomide to alpha1-acid glycoprotein may be involved in its inhibition of tumor necrosis factor alpha production. *Proc. Natl. Acad. Sci. U.S.A.* **1996**, *93*, 7552−7556.
(24) Woon, S.-T.; Baguley, B. C.; Palmer, B. D.; Fraser, J. D.; Ching, L.-M. Uptake of the antivascular agent 5,6-dimethylxanthenone-4-acetic acid (DMXAA) and activation of NF-kappaB in human tumor cell lines. *Oncol. Res*. **2002**, *13*, 95−101.
(25) (a) Bayley, H. Photogenerated Reagents in Biochemistry and Molecular Biology. In *Laboratory Techniques in Biochemistry and Molecular Biology*; Elsevier: Amsterdam, 1983; Vol. 12. (b) Knowles, G. Photogenerated reagents for biological receptor-site labeling. *Acc. Chem. Res.* **1972**, *5*, 155−160. (c) Sinz, A. Isotope-labeled photoaffinity reagents and mass spectrometry to identify protein−ligand interactions. *Angew. Chem., Int. Ed.* **2007**, *46*, 660−662.
(26) Brunner, J. New photolabeling and crosslinking methods. *Annu. Rev. Biochem.* **1993**, *62*, 483−514.
(27) Rewcastle, G. W.; Atwell, G. J.; Li, Z. A.; Baguley, B. C.; Denny, W. A. Potential antitumor agents. 61. Structure−activity relationships for in vivo colon 38 activity among disubstituted 9-oxo-9*H*-xanthene-4-acetic acids. *J. Med. Chem.* **1991**, *34*, 217−222.
(28) Atwell, G. J.; Rewcastle, G. W.; Baguley, B. C.; Denny, W. A. Relationships between structure and in vivo colon 38 activity for 5-substituted 9-oxoxanthene-4-acetic acids. *J. Med. Chem.* **1990**, *33*, 1375−1379.
(29) Rewcastle, G. W.; Sutherland, H. S.; Weir, C. A.; Blackburn, A. G.; Denny, W. A. An improved synthesis of isonitrosoacetanilides. *Tetrahedron Lett.* **2005**, *46*, 8719−8721.
(30) Baguley, B. C.; Calveley, S. B.; Crowe, K. K.; Fray, L. M.; O'Rourke, S. A.; Smith, G. P. Comparison of the effects of flavone acetic acid, fostriecin, homoharringtonine and tumour necrosis factor alpha on colon 38 tumours in mice. *Eur. J. Cancer Clin. Oncol.* **1989**, *25*, 263−269.
(31) Laws, A. L.; Matthew, A. M.; Double, J. A.; Bibby, M. C. Preclinical in vitro and in vivo activity of 5,6-dimethylxanthenone-4-acetic acid. *Br. J. Cancer* **1995**, *71*, 1204−1209.
(32) Ching, L. M.; Goldsmith, D.; Joseph, W. R.; Korner, H.; Sedgwick, J. D.; Baguley, B. C. Induction of intratumoral tumor necrosis factor (TNF) synthesis and hemorrhagic necrosis by 5,6-dimethylxanthenone-4-acetic acid in TNF knockout mice. *Cancer Res.* **1999**, *59*, 3304−3307.
(33) Ching, L. M.; Young, H. A.; Eberly, K.; Yu, C. R. Induction of STAT and NFkappaB activation by the antitumor agents 5,6-dimethylxanthenone-4-acetic acid and flavone acetic acid in a murine macrophage cell line. *Biochem. Pharmacol.* **1999**, *58*, 1173−1181.
(34) Woon, S. T.; Zwain, S.; Schooltink, M. A.; Newth, A. L.; Baguley, B. C.; Ching, L. M. NF-kappa B activation in vivo in both host and tumour cells by the antivascular agent 5,6-dimethylxanthenone-4-acetic acid. *Eur. J. Cancer* **2003**, *39*, 1176−1183.
(35) Wang, L. C.; Reddy, C. B.; Baguley, B. C.; Kestell, P.; Sutherland, R.; Ching, L. M. Induction of tumour necrosis factor and interferon-gamma in cultured murine splenocytes by the antivascular agent DMXAA and its metabolites. *Biochem. Pharmacol.* **2004**, *67*, 937−945.
(36) Ching, L. M.; Finlay, G. J.; Joseph, W. R.; Baguley, B. C. In vitro methods for screening agents with an indirect mechanism of antitumour activity: xanthenone analogues of flavone acetic acid. *Eur. J. Cancer* **1991**, *27*, 1684−1689.
(37) Woon, S.-T.; Reddy, C. B.; Drummond, C. J.; Schooltink, M. A.; Baguley, B. C.; Kieda, C.; Ching, L.-M. A comparison of the ability of DMXAA and xanthenone analogues to activate NF-kappaB in murine and human cell lines. *Oncol. Res*. **2005**, *15*, 351−364.
(38) Ching, L. M.; Joseph, W. R.; Zhuang, L.; Atwell, G. J.; Rewcastle, G. W.; Denny, W. A.; Baguley, B. C. Induction of natural killer activity by xanthenone analogues of flavone acetic acid: relation with antitumour activity. *Eur. J. Cancer* **1991**, *27*, 79−83.
(39) SibTech, Inc. http://www.sibtech.com.
(40) Bizouarne, N.; Mitterrand, M.; Monsigny, M.; Kieda, C. Characterization of membrane sugar-specific receptors in cultured high endothelial cells from mouse peripheral lymph nodes. *Biol. Cell* **1993**, *79*, 27−35.
(41) Mosmann, T. Rapid colorimetric assay for cellular growth and survival: application to proliferation and cytotoxicity assays. *J. Immunol. Methods* **1983**, *65*, 55−63.
(42) Bradford, M. M. A rapid and sensitive method for the quantitation of microgram quantities of protein utilizing the principle of protein−dye binding. *Anal. Biochem.* **1976**, *72*, 248−254.
(43) Sen, R.; Baltimore, D. Inducibility of [kappa] immunoglobulin enhancer-binding protein NF-[kappa]B by a posttranslational mechanism. *Cell* **1986**, *47*, 921−928.

JM0702175